sustainability

MDPI

Review

Recent Developments in Thermoelectric Generation: A Review

Daniel Sanin-Villa

Instituto Tecnológico Metropolitano, Medellín 050036, Colombia; danielsanin@itm.edu.co

Abstract: The world's growing energy demand poses several concerns regarding the rational and efficient use of energy resources. This is also the case for many industrial processes, where energy losses and particularly thermal losses are common. Thermoelectric generators offer an alternative to address some of these challenges by recovering wasted heat and thereby increasing the overall efficiency of these processes. However, the successful operation of the thermoelectrical modules meant to carry this process is only possible when pairing these to an external control system; such a system plays an important role in predicting and operating such modules at its maximum power point. In this review paper, recent developments in the field of thermoelectric technology are discussed along with their mathematical models, applications, materials, and auxiliary devices to harvest thermal energy. Moreover, new advancements in phenomenological models are also discussed and summarized. The compiled evidence shows that the thermal dependence properties on the thermoelectric generator material's modules and the mismatching thermal conditions play an important role in predicting power output in those systems, which prove the importance of including those parameters to enhance the accuracy of the energy production prediction. In addition, based on the evaluation of the mathematical models, it is shown that more studies are required to fill the gap between the current state-of-the-art of the technology and adjacent modeling techniques for the design and evaluation of thermal energy harvesting systems employing thermoelectric arrays under mismatching thermal conditions.

Keywords: thermoelectric generator; phenomenological models; mismatching thermal conditions

Citation: Sanin-Villa, D. Recent Developments in Thermoelectric Generation: A Review. *Sustainability* **2022**, *14*, 16821. https://doi.org/10.3390/su142416821

Academic Editor: Kian Jon Chua

Received: 18 November 2022
Accepted: 10 December 2022
Published: 15 December 2022

1. Introduction

Humanity's increased energy usage continues to be of concern. In 2015, several countries signed the Paris Agreement and thereby committed to a series of actions targeted to slow down the current global warming rate. [1]. That objective can only be achieved by performing a series of actions focused on energy efficiency, reducing CO_2 emissions, and increasing renewable energy usage [2]. Among the options to improve the energy efficiency in processes, different initiatives are proposed to take advantage of waste heat sources; in Turkey, for instance, about 51% of the total heat used in the industry is wasted [3]. In other developed countries such as France, it is estimated that 30% of the thermal energy is not used [4]. For this purpose, several investigations have focused their efforts on developing new materials with thermoelectric properties, which can take advantage of temperature gradients for the generation of electrical energy in a direct way. These materials are semiconductors that generate a difference in electrical potential when they are subjected to temperature gradients [5], using the Seebeck effect.

The analysis of thermoelectric generators (TEG) systems covers different research areas where modeling is one of the most interesting; mathematical models allow for the prediction of the performance of a TEG system in terms of energy production and support the development of efficient designs, new materials, and alternative control systems, among others. The modeling of TEG systems requires a set of concepts such as heat transfer and electric conductance models, external circuital elements, environmental conditions effects, and thermal energy sources to extract the power. To successfully perform this, it

is important to consider the thermal effect over material properties in semiconductors, which could cause a difference between the predicted values and experimental results, leading therefore to inaccurate analysis and causing a significant reduction in the efficiency of energy production systems. This paper is focused on reviewing recently conducted research for the development of a modeling technique to design and evaluate energy harvesting in TEG systems.

In the following section, the concepts and theoretical framework around energy production in thermoelectric systems are explained briefly. Afterward, an overview of several applications and industrial systems is performed, followed by a summary of the new developments in thermoelectric materials and their performance parameters. Finally, recent advances in mathematical models with complex methods, including the material's thermal dependence properties, are outlined. The last section summarizes the main problem regarding the mismatching condition in interconnected cells and finally, this review paper also presents suggestions for future studies in the field.

2. Theoretical Framework

2.1. Overview of Thermoelectric Generators

Italian scientist Alessandro Volta first observed heat conversion into electricity in 1794 [6]; he conducted an experiment where an iron bar with two ends at different temperatures created enough energy to activate the spasm of a frog's leg. In 1823 this phenomenon was rediscovered by Thomas Johann Seebeck, who joined two wires of different materials and perceived a magnetic effect when the magnetic field turned a compass needle toward the pair of cables; Seebeck continued investigating these pairs, known as thermocouples [7]. Subsequently, Danish scientist Hans Christian Ørsted ratified Seebeck's experiments and defined this term as thermoelectricity. After the discovery of the Seebeck effect in 1834, Jean Charles Athanase Peltier found that by passing an electric current through a thermocouple, it is possible to transfer heat from or to the surroundings [8]. One of the main advantages of thermoelectric devices is the absence of moving parts and its low electricity costs; however, several parameters affect the performance of these systems, including the materials, phenomena that can occur inside each module, module configurations, maintenance, operative conditions, and mismatching energy source, among others. Thermoelectric devices are operated in two different modes: thermoelectric cooling modules (TEC) and thermoelectric power generator (TEG). TEC modules work when electrical current flows through the device and the device transports energy (heat) from one side to the other. When the module receives heat from one side, and no current is forced into it, a difference in temperature is created between both sides and, then, the device works as a TEG and transforms part of the heat into a Direct Current (DC) voltage.

Thermoelectric cooler devices have been widely used where the conventional cooling mechanisms are not available or difficult to implement; the TEC are solid-state devices with high reliability, compact packaging, and low weight [9]. Söylemez et al. developed and evaluated hybrid refrigerators, which include vapor compression and thermoelectric cooling; the test results showed that the hybrid refrigerators had at least three times higher energy consumption levels over the serial ones due to lower operating efficiencies of the TECs and higher transmission losses [10]. Yuan Wang et al. presented a model to establish the energy conversion efficiency of an alkali metal thermoelectric converter (AMTEC) by combining it with an absorption refrigerator (AR) [11]. Finally, in 2011 Zheng et al. presented a review of TEC in vehicular heating and cooling, medical service, the food industry, and electronic devices [12].

The TEG modules are used in diverse and specialized applications such as military, aerospace, and automotive equipment; Daniel Champier in 2017 presented a critical review of different TEG applications [13].

To obtain information about energy production and efficiency performances under different operating conditions, analytical and numerical methods have been used, commonly supported by experimental data. Modeling a TEG is not a trivial task, it is necessary

to consider different elements and conditions that could affect the behavior realistically and practically. To represent the physical phenomenon occurring in a Thermoelectrical module (TEM), both thermal and electrical circuits should be driven. The most adopted approaches consider that a TEM consists of a P–N junction connected electrically in series and thermally in parallel. A one-dimensional (1-D) representation of the TEM allows for the determination of analytical expressions of heat absorbed and heat rejected, where the power output is defined as the difference between heat absorbed and heat rejected. Figure 1 presents the P–N array (of N legs) inside a TEM, where T_H, Q_H, and K_H are, respectively, the heat source temperature, heat supplied from a heat source, and thermal conductance from the hot side of the TEM. On the opposite side T_L, Q_L, and K_L refer, respectively, to heat sink temperature, heat rejected from the module to heat sink, and thermal conductance of the cold side. α, k, and ρ are defined as the Seebeck coefficient, thermal conductivity, and electrical resistivity.

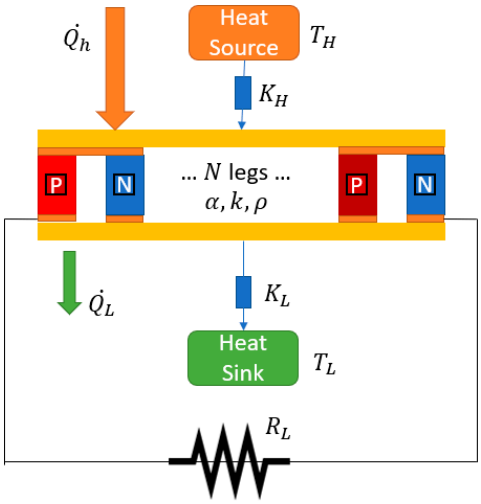

Figure 1. One-dimensional representation of a TEM.

The electrical resistance network presented in Figure 2 shows the connections of N legs (P and N type) in series through conductive material tabs. It shows that a TEG system can be modeled as a voltage source (V) in series with a TEG internal resistance.

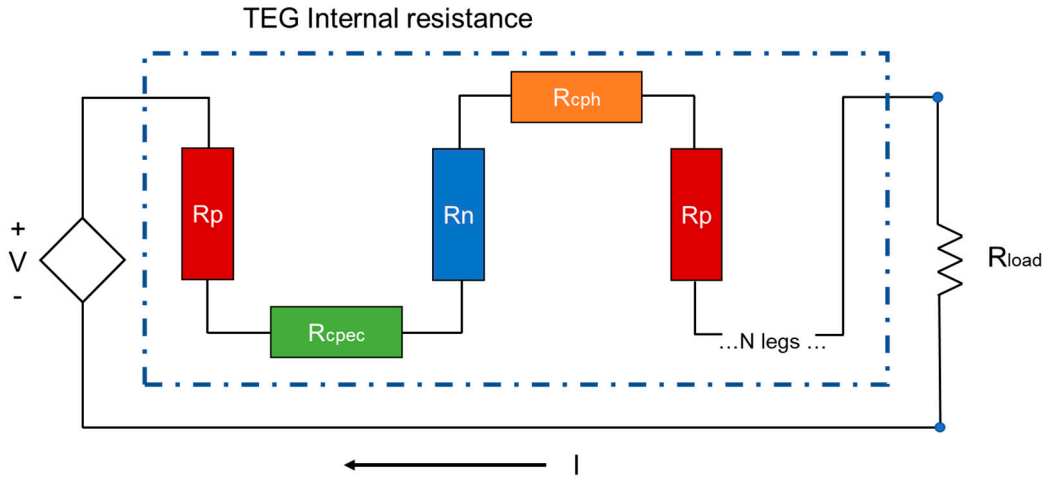

Figure 2. Electrical representation of a TEM.

The R_p and R_n are electrical resistance associated with P and N type semiconductor legs, respectively. R_{cpec} and R_{cph} are the electrical resistance of material-conductive strips on the hot side, the electrical resistance of material-conductive strips on the cold side, respectively, and R_{Load} correspond to the external load resistance.

Figure 3 shows a 3D view of a thermoelectric generator in a flat plate geometry; the filler and the thermal interface layer (TIL) could vary according to the application (this is just a general representation of a TEG module).

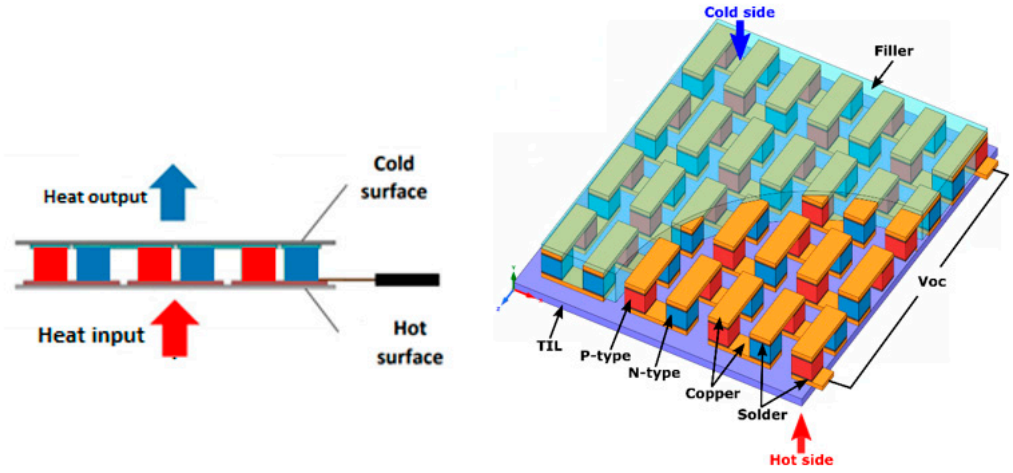

a) Lateral side of a thermoelectric module. b) Elements in a TEG Module.

Figure 3. Typical element configuration in a flat thermoelectrical module (TEM). (**a**) Lateral view of the thermoelectric module; (**b**) Material elements on thermoelectric modules.

The module in Figure 3 consists of two types of semiconductors: positive (P-type) and negative (N-type), where the P-type has surplus holes, and the N-type is carried by negative charges (electrons) to carry the thermoelectric current. The electrons move from one leg to another when the heat flows from the hot surface to the low-temperature surface; this movement converts the heat flux into electrical energy and produces power to interact with an electrical load.

2.2. The Onsager Relationships

In 1930, Lars Onsager published his famous work "Reciprocal relations in irreversible processes" [14], which was one of the most ingenious ways to describe the interference of two (or more) irreversible and simultaneous transport processes (i.e., heat and electrical conduction). When two different materials are coupled and an electric current pass through the junction, absorption of heat occurs and it is called the Peltier Effect. On the contrary, if two opposite junctions are maintained at different temperatures, an electromotive force (voltage) will appear in the circuit. Onsager presented a practical way to understand, in general, the coupled effect under the hypothesis of a linear response between the fluxes and forces responsible for the simultaneous transport phenomena. Equation (1) is presented as follows:

$$J_k = \sum_j L_{jk} F_j \quad (1)$$

where J_k represents the flux, F_j is the driven forces, and L_{jk} are the phenomenological coefficients. According to the Curie principle [15], for isotropic systems, symmetries concerning the phenomenological coefficients lead to fluxes that will not be dependent on all the possible forces, i.e., currents and forces of differing tensorial order will not interact with each other. The Onsager's reciprocity relations present symmetry among thermodynamic cross-effects, the j-th general force takes place in the creation of the k-th flux just with the same weighting factor as the k-th force. Mathematically, it is easy to show according to Equation (2):

$$L_{jk} = L_{kj} \quad (2)$$

2.3. The Seebeck Effect

The principle of a TEG module is the Seebeck effect. When a thermoelectric coupled has a heat source, and it applies heat energy to create a temperature difference between both sides of the P–N couple, an electrical current is induced in the circuit, and that electric current indicates that a voltage is created due to the movement of heat. In 1794, Alessandro Volta discovered this phenomenon, but thanks to T.J. Seebeck's works on thermoelectric forces, the effect adopted his name [16]. The Seebeck coefficient, $\alpha(T)$, can be expressed according to Equation (3):

$$\alpha(T) = -\text{grad}(\varphi)/\text{grad}(T) \quad (3)$$

Here, φ represent the voltage, T temperature, and $\alpha(T)$ is the combined coefficient related to material Seebeck properties used in P–N coupled. Usually, $\alpha(T)$ of the junction between two materials is the difference between the two absolute parameters properties of each material.

2.4. The Peltier Effect

The principle of a TEG Opposite to the Seebeck effect, the junction of two different isothermal materials with an electron current flow across them, produces a heat rejection or absorption according to the current direction. Usually, the Peltier effect is explained by the change in the average kinetic energy of a charge carrier (the electron) when the junction is crossed [17]. Equation (4) shows the Peltier coefficient (π) as the relation between the heat transfer rate from the union (Q) and the current flowing through them (I).

$$\pi = Q/T \quad (4)$$

2.5. The Thomson Effect

In 1854, William Thomson (Lord Kelvin) discovered that there is an extra reversible heat flux in excess of the Joule dissipation heat when a homogeneous material is exposed simultaneously to a thermal gradient and an electric current flow. The thermodynamic analysis for TEG, including this effect, has been widely presented. Zhang et al. [18] analyzed the influences of the Thomson effect on the power output of a thermoelectric generator; they found the difference between the conversion efficiencies with the Thomson effect, and, without the Thomson effect, it increases fast with the temperature difference between the hot and cold ends. This effect has also been studied in different leg geometries [19,20]; the authors concluded the Thomson effect lowers the performance of a thermoelectric generator. The Thomson coefficient can be related to the Seebeck coefficient through Equation (5).

$$\tau(T) = T\ (\delta\alpha/\delta T) \quad (5)$$

3. Applications of Thermoelectric Generators

One of the most promising areas where TEG could adopt an important role is "The Internet of things" (IoT), developments in predictive maintenance, and using a wireless signal from monitoring variables to predict and schedule important tasks [21]. The power source of the IoT sensors usually comes from batteries; here, the TEG device could improve these technologies with constant energy provided from industrial waste heat, which is available in most industrial equipment. Cataldo et al. [22] present an evolution timeline of power generators in space exploration; one of the most used are the radioisotope thermoelectric generators (RTGs) that do not use nuclear fission or fusion but the heat from the natural radioactive decay of radioactive material such as plutonium-238. Hundreds of radioisotope heater units have been launched in different space missions, providing thermal energy to critical components on missions such as the Apollo 11 and Pioneers 10/11, Voyagers 1/2, Galileo, and Cassini. Thermoelectric devices used in industrial applications have been studied using heat wasted or a byproduct of the process. In general, the waste heat is reused with conventional thermal cycles, such as ORC [23] or TRC [24,25]. However, TEG systems have been studied under industrial conditions. Ramirez et al. [26] investigates

the performance of a thermoelectric generator with 20 modules by implementing a waffle heat exchanger; the experimental results showed a variable range of power recovery from 57.87 W to 71.13 W. Khalil and Hassan in 2019 proposed an effective way to improve waste heat recovery from chimneys using thermoelectric generators cooled by natural convection heat sinks. A modified heat sink equipped with a flap fixed at the top of its base is used instead of only the conventional heat sink; this modification increases the output power by about 64% [27]. Aranguren et al. [28] built a TEG prototype located at the exhaust of a combustion chamber, provided with 48 modules obtaining 21.56 W in an area of 0.25 m^2 of usable energy; they also analyzed the influence of the gas temperature and mass flows, finding as expected, that higher values of those parameters produce higher thermoelectric power. Qui Luo et al. [29] proposed a TEG waste-heat-recovery system to reduce heat losses from cement rotary kilns, using a Bi_2Te_3–PbTe hybrid system that generates around 211 kW electric power, recovering more than 32.85% of the lost thermal energy.

Kaibe et al. [30] developed a TEG at a carburizing furnace of Komatsu Ltd., Tokyo, Japan; they used 16 Bi_2Te_3 modules and a heat exchanger, which collected approximately 4 kW. The maximum electrical output power was around 214 W, which represents an efficiency of 5%, but the power used to cool the cold side of the modules was not included in these results. Kajihara et al. published a series of works [31–33] where a TEG system was implemented in a JFE Steel Corporation (JFE), with a 10-kW grid-connected TEG system for JFE's continuous casting line with a KELK Ltd., Hiratsuka, Japan, generating electric power using radiant heat from a continuous casting slab. Kurokit et al. [32] used 56 Bismuth-Telluride TEM with a maximum operating temperature of 553 K at the high-temperature side and a maximum of 423 K at the low-temperature side. They presented a simple model [31] to calculate the heat crossing through the modules and estimate the maximum power output. In Equation (6), r_e is the internal electrical resistance and ΔT the difference between hot and cold side temperatures.

$$P_{max} = (\alpha \Delta T)^2/(4r_e) \quad (6)$$

On the opposite scale, microsensors and small measurement devices can operate using TEG as an energy source, reducing the inconvenience of using long cables or static locations. Batteries are widely used for those purposes, but their lifetime is generally shorter than the designed operational time of sensors. One practical solution is a microgenerator with no maintenance requirements; in many factories, heat sources are available. The company Microplet [34] developed a small TEG device that can generate from 1 mW to 40 mW with temperature differences between 10 °C and 30 °C. They connected hundreds of P–N thermocouples in series to obtain a higher voltage that is easy to convert with commercial DC/DC power converters. Perpetua [35] developed a TEG for sensors powered by temperature differences that already exist on surfaces of equipment such as pipes, pumps, fans, and motors; their device includes the internal electronics needed to store and regulate the renewable energy and deliver a regulated voltage to transceivers and sensors; they reported sacksful cases from different industries such as steel manufacturing and oil and gas companies. Kim et al. [36] developed a TE of 140 mm × 113 mm and produced 272 mW of energy from a heat pipe at a temperature of 70 °C, this system was used to remotely monitor the heat pipe temperature, ambient temperature, humidity, CO_2, and volatile organic compound concentrations. Milic' et al. [37] characterized different commercial TEG for wireless sensors and found they can be selected based on the power generation, figure of merit, or thermocouple legs length. Guan et al. [38] proposed a two-stage boost scheme system to harvest thermal energy and run a microcontroller unit and a wireless sensor node under low input voltage and power with high efficiency, reaching an open circuit voltage of 62 mV and input power of 84 μW.

The TEG for human energy harvesting is also studied; power generation application over human-body skin requires the use of flexible and biocompatible substrate since the human body is not a flat surface. Some fabrication techniques include electro-deposition, screen printing, screen printing, and inkjet printing [39]. Some problems of human body

harvesting are the thermal contacts between TEG and human skin and the natural air convection, which allows a small temperature difference and low power energy is extracted. Wang et al. developed a numerical model to investigate the performance of wearable TEGs on the curved human wrist; they analyzed the impact of curvature in power generated and found the impact was low [40]. Hylan et al. [41] tested a TEG on different body locations, comparing the energy produced on each, and found the highest to lowest power generated was on the upper arm, wrist, chest, and T-shirt, respectively. Siddique et al. [42] fabricated two TEG prototypes for human harvesting using a manual dispenser printing technique; both elements were tested and found to be very flexible, twistable, and durable, the power output was extremely low between 2.2 and 3.1 nW. Many other applications of energy harvesting using thermoelectric materials have been developed in other fields such as aerospace [43–45] and marine [46–48] industries.

4. Materials in TEG Performance

To achieve higher efficiencies, different thermoelectric materials have been studied, from metal to ceramics, semiconductors, and certain polymers, which exhibit interesting thermoelectrical properties. The performance of TEG is highly related to the material's properties; in Equation (7), the dimensionless Figure of Merit (ZT) is used as a performance parameter.

$$ZT = (\alpha^2 \sigma / (k_e + k_{th}))\, T \quad (7)$$

where σ is the electric conductivity, k_e thermal conductivity due to electron transport, and k_{th} the thermal conductivity due to the lattice phonon [49]. High values of ZT imply the higher performance of TEG modules; the best TE material would be those with higher electrical conductivity and lower thermal conductivity, this is phonon-glass electron crystal materials (PGEC) [42,49–56]. According to the Wiedemann–Frenz law, the k_e is proportional to σ and temperature by a factor of L (Lorenz factor), which is an interesting challenge to design new material with higher values of ZT. Most efforts have been focused on reducing the lattice thermal conductivity (k_{th}) [57] to increase the figure of merit. Therefore, the ZT variables are interrelated and require careful optimization of the material properties to improve it.

Bismuth telluride (Bi_2Ti_3) has been widely used due to its relatively higher commercial value than other available thermoelectric materials, but its power–cost rate can reach as high as 1.1 kW/USD 10,000 [58]. Nanostructured materials have been developed in recent years to achieve higher performance reducing the lattice thermal conductivity and improving electrical transport performance [59–61].

Cai et al. [62] classified the TE materials in three categories:

- Traditional TE materials: including Bi_2Ti_3-based alloy for low-temperature applications, PbTe for mid-to-high temperatures, and SiGe alloys for higher temperatures (up to 1275 K).
- Major materials except the traditional: skutterudites materials ($CoSb_3$ alloy—their structure is composed of eight corner-shared $CoSb_6$ octahedrons), Mg_2Si, higher manganese silicides (HMS), half-Heusler compounds (intermetallic *M*NiSn and *M*CoSb where *M* could be Ti, Zr or Hf), and Zintl compounds (metals with a larger difference in electronegativity).
- Sulfides and selenides: Sn*X* where *X* could be Se or S; Cu_2X where *X* could be Se or S; and $Cu_{12}Sb_4S_{13}$ tetrahedrite.

Different fabrication methods for designed engineering material techniques have been developed to increase the figure of merit ZT in TE materials. The highest value found in the literature review was reported by Chang et al. in 2018 (ZT = 2.8) [63] in a Br-doped SnSe single crystal. Table 1 present a list of different TE materials and their maximum ZT values achieved.

Table 1. Revision of figure of merit for different TEG materials.

Material	Max. ZT	Reference
Nanocrystalline BiSbTe	1.40 @ 373 K	[64]
$Bi_{0.48}Sb_{1.52}Te_3$	1.50 @ 390 K	[65]
$Bi_{0.5}Sb_{1.5}Te_3$	1.30 @ 273 K	[66]
$Bi_{0.5}Sb_{1.5}Te_3$	1.86 @ 320 K	[67]
Polycrystalline BiSbTe alloys with nanodiamond inside	1.25 @ 323 K	[68]
PbTe Tl doped	1.50 @ 773 K	[69]
PbTe Zn n-type doped	0.80 @ 800 K	[70]
AgPbmSbTem+2	1.54 @ 723 K	[71]
PbTe Na-doped	1.70 @ 740 K	[72]
$Na_{0.03}Eu_{0.03}Sn_{0.02}Pb_{0.92}Te$	2.60 @ 800 K	[73]
$Si_{95}Ge_5$ with nano $Si_{70}Ge_{30}P_3$	1.30 @ 900 K	[74]
$Si_{80}Ge_{20}$-SiO_2 nanoinclusions	0.72 @ 800 K	[75]
$CoSb_3$ with nano Yb_2O_3	1.60 @ 835 K	[76]
$Mg_2Si_{1-x}Snx$	1.30 @ 700 K	[77]
$Mg_2Si_{0.4-x}Sn_{0.6}Sb_x$, x = 0.0075	1.10 @ 773 K	[78]
$Hf_{0.25}Zr_{0.75}NiSn_{0.97}Sb_{0.03}$	1.00 @ 900 K	[79]
Zn_4Sb_3	1.35 @ 380 K	[80]
Mg_3Sb_2 Mn doped	1.85 @ 723 K	[81]
Br-doped SnSe single crystal	2.80 @ 773 K	[63]
Polycrystalline SnSe	2.10 @ 873 K	[82]
Cu_2Se in phase transition region	2.40 @ 1000 K	[83]

The most common thermoelectric materials used in industrial TEGs are inorganics, such as bismuth telluride (Bi_2Te_3), silicon–germanium (SiGe), and lead telluride (PbTe) and its alloys [84]. Bi_2Te_3 is the most widely used because of its relatively better thermoelectric efficiency near room temperature [85]. Many examples in the research have been developed around the objective of increasing TE efficiency with the improvement of thermoelectric properties such as the thermal conductivity and the Seebeck coefficient [86–88]. Inorganic materials are limited by their high prices, rare elements raw materials, complex manufacturing processes, and low flexibility for mobile and human energy harvesting applications [89].

On inorganic TE material, such as PbTe- or BiTe-based alloys, n-type materials have been studied to increase their TE performance because of their strong anisotropy carrier transport [90]. The enhancement of n-type inorganic material is addressed mainly by two mechanisms: dynamic doping to optimize n for increasing electric conductivity [91] and engineering the band structure to increase the Seebeck coefficient [92]. Yang et al. [93] developed a composite strategy to improve both the TE and mechanical performance of n-type materials with Bi-Te-Se by incorporating carbon microfibers. Mo et al. [94] optimize the performance of n-type $Mg_{3.2}Bi_{1.4}Sb_{0.6}$-based material by adding Se as an electron dopant. The mid-to-high PbTe materials have significantly high thermoelectric performances, with figures of merit higher than one, with Bi-doped PbTe [95] and Bi-doped PbTe/Ag2Te Nanocomposite [96].

N-type polymers have less TE performance than the p-type polymer elements, with a difference in electric conductivity and power factors of 100 and 50 times, respectively [97]. To improve the TE performance of n-type polymers, researchers have modified their chemical composition [98], designed novel conjugated polymers [99], structural modulation and doping engineering [100], and worked on more efficient dopants to increase electric conductivity for enhanced electron density [101].

Relevant characteristics of TE organic materials are their low cost, lower density, high flexibility, and, in some cases, higher performance at ambient temperature [102]. Research, including on carbon nanotubes/polyaniline composite films, has found interesting results due to its low thermal conductivity [103]; the main problem for TE polymer materials is the difficulty of dissolving it in organic solvents, but the electrochemical deposition process is a practical solution to address this issue [104]. Research on polypyrrole [105,106],

polyaniline [107,108] and poly:poly composites [109–111] materials has been conducted. Carbon nanotubes also show interesting results because of their TE and mechanical properties [112]; additionally, Blackburn et al. [113] have previously summarized the advantages of carbon-nanotube (CNT)-based thermoelectric materials such as cost-effectiveness, ease of fabrication, flexibility, stretchability, and them being lightweight, but further research is needed to develop and improve the doping, functionalization, and stabilization of those materials; they also found it promising to achieve a TE power factor greater than one in the next decade. Elsehly et al. [114] found that the annealing effect on multiwall CNTs can increase the electrical conductivity and Seebeck coefficient while significantly decreasing the thermal conductivity; the TE performance was evaluated over the temperature range of 300–450 K.

5. Mathematical Models of TEG Devices

One of the main interest topics of this proposal is to develop a phenomenological model for a TEG system, so an analysis of published works on this is presented in this section. The main developments and conclusions of the results studied are introduced in this section to recognize the key points of the current research in the modeling of TEG systems. The study of these phenomena, from irreversibility analysis, allows for the determination of the best design conditions and efficiency and to maximize the electrical power output [115]. In 2014, Tzeng et al. developed a parametric study for heat transfer in a thermoelectric generator, the one-dimensional heat conduction model included both the Seebeck effect and the generation of heat due to the Joule effect [116]. Some researchers have included the analysis of these phenomena solving the equations through finite differences, including in the models the Seebeck, Thomson, Peltier, and Joule effect, finding that the inclusion of the Thomson effect has an important role in the accuracy of the formulated models [117]. Among the phenomena mentioned above, the heating due to the Joule effect, which is considered thermodynamically irreversible [118], and other assumptions and considerations, it is possible to separate the phenomenological models into two large groups for the analysis of thermoelectric devices: simplified models and complex models. The simplified models macroscopically analyze the phenomenon, creating global thermoelectric balances; in many cases, these models disregard the presence of the Thomson effect [119,120] mainly because they consider the value of the Seebeck coefficient as an independent parameter of the temperature. In these models, the properties of the materials are determined from the average temperatures of the cold and hot surfaces and this assumption is made in the vast majority of investigations reviewed to date. On those cases, the heat flux and power generation equation for TEG modules becomes [121–124]:

$$Q_H = \alpha_{avg} I T_H + K_{avg} \Delta T - R_{avg} I^2/2 \quad (8)$$

$$Q_L = \alpha_{avg} I T_L + K_{avg} \Delta T + R_{avg} I^2/2 \quad (9)$$

where

$$R_{avg} = L/\sigma A \quad (10)$$

$$K_{avg} = kA/L \quad (11)$$

R_{avg} is the electrical resistance and K_{avg} the thermal conductance. The power output is computed according to Equation (12)

$$P = \alpha_{avg} \Delta T I - R_{avg} I^2 \quad (12)$$

Some studies present an improvement of the model, including the Thomson effect, where it is distributed on the two sides of the TEG module equally. In those models, the Thomson effect compensates the Joule effect ([18,125]).

$$Q_H = \alpha_{avg} I T_H + K_{avg} \Delta T - R_{avg} I^2/2 - \tau I \Delta T/2 \quad (13)$$

$$Q_L = \alpha_{avg} I T_L + K_{avg} \Delta T + R_{avg} I^2/2 + \tau I \Delta T/2 \quad (14)$$

The electrical power, including the Thomson effect, yields:

$$P = \alpha_{avg} \Delta T I - R_{avg} I^2 - \tau I \Delta T \quad (15)$$

The complex models more precisely describe the TEG by using local balance equations, including the mass, energy, and entropy equations [126,127]. Some works present energy evaluation on steady-states [6,128–130], but others present transient models [99] according to the following energy balance in Equation (16):

$$\rho C_p (\delta T/\delta t) = \text{div}(k \, \text{grad}(T)) + J^2/\sigma - \tau J \Delta T \quad (16)$$

In rare cases, the models including temperature-dependence properties have been carried out. Musland et al. [131] implement the Landauer formalism approach with ballistic quantum transport equations to calculate thermoelectric transport properties as follows:

$$\sigma = \int dE \sum(E) F_T(E) \quad (17)$$

$$\alpha = -(1/\sigma eT) \left(\int dE \sum(E) F_T(E) (E - \mu) \right) \quad (18)$$

$$K = (1/e^2 T) \left(\int dE \sum(E) F_T(E) (E - \mu) - T\sigma\alpha^2 \right) \quad (19)$$

Also, in this model, it is necessary to know $\sum(E)$, often referred as the transport distribution function and $F_T(E)$, which is the thermal broadening function or Fermi window:

$$F_T(E) = -\delta f(E)/\delta E \quad (20)$$

where f(E) is the Fermi function.

Yamashita analyzed the TEG efficiency considering the linear and non-linear (second-order) temperature dependence of material properties [132] and found that the non-linear component in the temperature dependence of the Seebeck coefficient among other TE properties has the greatest effect on efficiency, but no heat losses were considered. Wee [133] presented a comparison study to understand the effects on the linear and second-order relationship between thermoelectric properties and temperature over TEG devices, including the Joule heat and the Thomson effect; in this work, he excluded the contact resistances at the ends of the thermoelectric element and the heat loss from the side walls of each thermoelectric element; it is also demonstrated that the appropriate consideration of the Thomson effect is essential in describing TEG behavior. Ju et al. [134] proposed an approximate analytical solution for a properties temperature dependence model evaluating the distribution of the electric resistivity and Thomson coefficient linearly and the distribution of electric resistivity and Thomson coefficient with a non-linear relationship; additionally, they neglected the thermal losses from thermocouples sides and found that thermal conductivity is a critical factor on the improvement of TEG efficiency. Lee et al. [104] considered radiative and conductive thermal losses using effective material properties; they concluded that a comparison of effective material properties and averaged material properties showed that thermal losses and interfacial resistance reduce efficiency significantly and that the utilization of the effective properties accounted for most parasitic losses by a straightforward increase in thermal conductivity and therefore a decrease in the figure of merit. In another study, Wee [135] also presented a PCE (polynomial chaos expansion) technique to quantify the uncertainties in the performance indices of TEG due to the uncertain material properties; he concludes that even the first-order polynomial approximation model performs accurate results (due to its low energy conversion efficiency), such an approximation will not be useful for the further development of novel TE materials with higher efficiency.

T. Zhang [136] studied the dependence of TEG properties as a function of temperature in four different thermoelectric materials, finding large differences in temperature distribution between the results reported by the models that use constant properties and those predicted by those including variable properties. Despite the clear relationship between temperature and material properties, some investigations conclude that it is possible to quantify performance parameters using effective property values efficiently and practically, with no need to analyze their temperature dependence [17]. However, due to the nonlinearity caused by thermal dependence properties, the complex model has not been fully developed and they are presented as an opportunity for future work [137]. As far as the authors' best knowledge, a complex model including temperature dependence material properties and side-leg heat losses due to convection and radiation has not been developed.

6. TEG Systems under Mismatching Conditions

In general, the TEG supplies low voltage or current levels [138]; one way to increase those values is to array several thermoelectric modules (TEM) into an array (serial, parallel, or a combination of both). In applications where high values of voltage and power are required, it is necessary to connect a high number of TEM in chains of series circuits and a group of a chains in parallel to create an array with enough power output. Figure 4 shows an example of different TEM in an array.

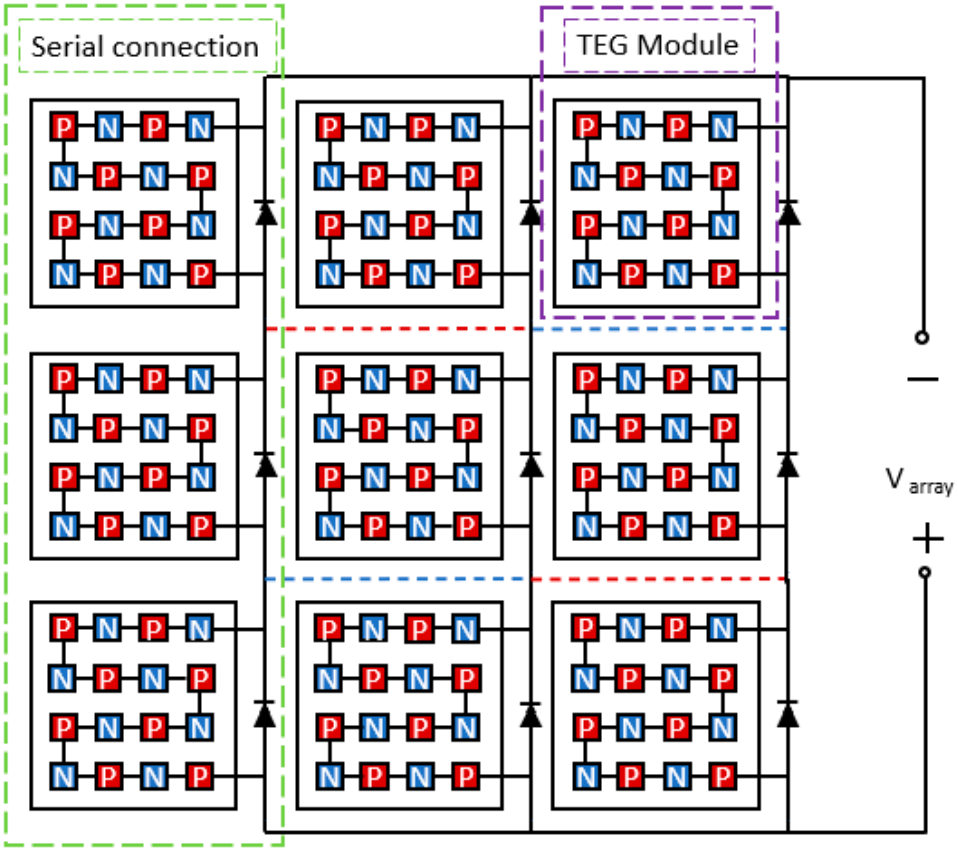

Figure 4. An array of thermoelectrical modules under different configuration (serial and/or parallel) modes.

The characteristic operative curves for commercial TEG under uniform conditions (the same temperature gradient) are presented in Figure 5. It can be easily noticed that the curve has a maximum power point (MPP) at V_{MPP} and I_{MPP}.

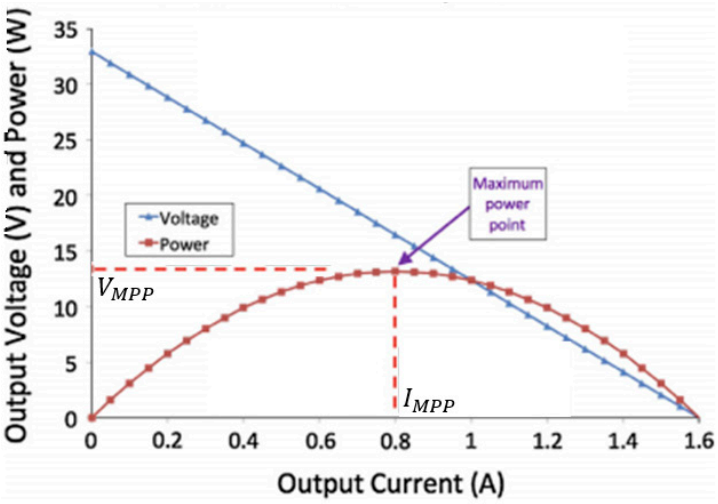

Figure 5. Electrical characterization (V–I and P–I curves) of the thermoelectric generator GM250-449-10-12 by European Thermodynamics Ltd., Harcourt, UK. Adapted from [108–110].

To obtain the maximum power from an arrangement, a DC–DC power electronic converter is necessary to reach that MPP; it is possible through different algorithms to track that point and extract the maximum power output (MPPT) such as the perturb and observe (PO), constant voltage (CV), and incremental conductance (INC) [139]. Those algorithms track the MPP using voltage and current measurements; several investigations propose different methods to reach that point rapidly and efficiently. According to Belboula et al., to maximize the power produced by the TEG, the electrical load impedance should be equal to the TEG's internal resistance [139–143].

The power provided by TEG systems depends directly on the temperature gradient, an ideal situation for modeling would be that all the modules of an array were exposed to the same temperature gradient; unfortunately, this condition is not always possible since the TEM arrays are usually exposed to different thermal conditions. Other situations such as the lack of maintenance, dust, and non-uniform heat sources could cause different temperature operating conditions between the modules. This is known as mismatching conditions and the main consequence is the difference in power output generated by each module inside the array.

Figure 6 illustrates an array of TEM under mismatching thermal conditions. The current generated by each module will be different under those circumstances, where one or more modules could produce higher current values than the others. If one of the high current modules is connected in a serial chain, the other modules will receive it, and that would force the other modules to gain an input current and to work improperly.

In photovoltaic (PV) arrays, a bypass diode (BD) is commonly used in an antiparallel configuration with the PV module. The BD is activated to let the current flow from the high-current PV modules and avoid the modules with lower energy production due to shade or dust [144]. Figure 6 presents the strategy applied to the TEG array: The B module has a lower energy generation than A module due to the mismatching condition, the current flow through the continuous line. When the BD in module B is activated, the energy produced by the module is not carried to the external load (i.e., a battery) and the total energy produced by the array will decrease.

The current flows through the BD because that path is the lower resistance line and the voltage in the TEM goes to zero; that is why the total power output added by the B TEM will be zero.

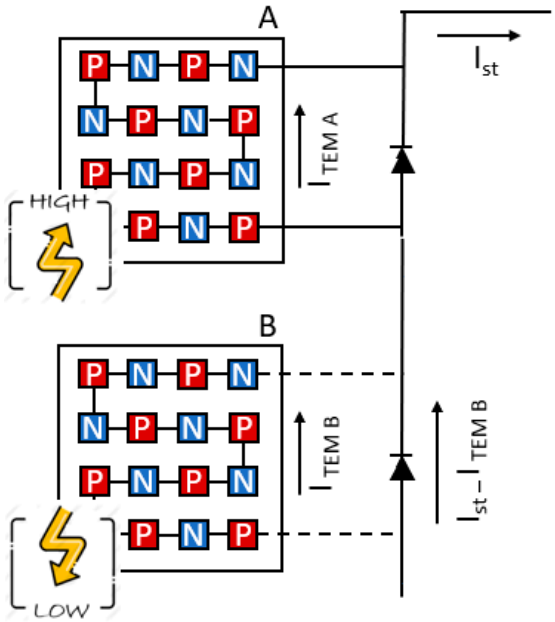

Figure 6. Connection of two different TEM under mismatching conditions. (**A**) high power generation. (**B**) low power generation.

The presence of the BD and its activation could cause multiple local peaks in the Voltage Power curve (local MPP) and the MPPT control algorithm could not find the global maximum power point (GMPP). However, some control techniques have been developed for PV systems where similar situations occur. Montecucco et al. [138] studied the effect of temperature mismatch on thermoelectric generators electrically connected in series and parallel, identifying that the mechanical clamping pressure of an individual TEG module could cause a significant mismatching condition. In their model, the TEG array is presented as a voltage source and a serial resistance, according to Figure 7.

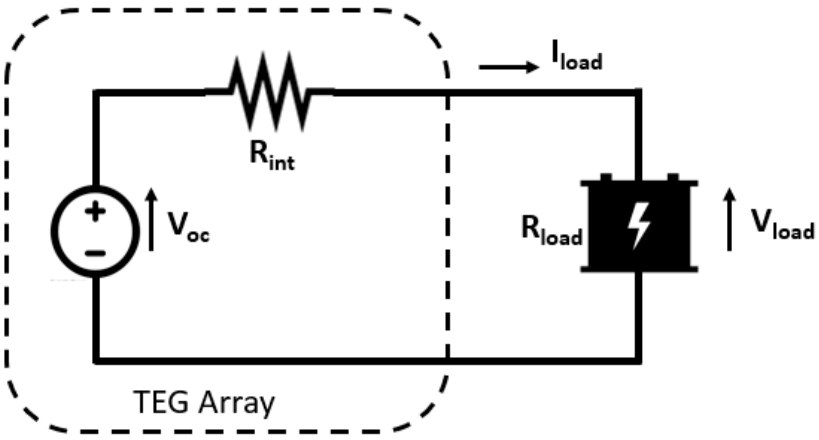

Figure 7. Circuital representation as a voltage source of a TEG array.

To analyze the array configuration, Montecucco et al. tested one TG module and an empirical voltage correlation was obtained according to Equation (21), where a, b, c, d, e, and f where determined from the experimental results for different temperature gradients ΔT [138].

$$V = (a\Delta T^2 + b\Delta T + c) - (d\Delta T^2 + e\Delta T + f) \quad (21)$$

Tang et al. [145] studied the impact of thermal mismatching on the output electrical power for automotive waste heat recovery systems experimentally; they found a decreased power output under mismatched temperature conditions; and they also concluded that a

proper mechanical pressure applied on the modules improves the electrical performance. The experimental results show that the power loss of the modules in a series connection is significant, reaching 11% less than the theoretical maximum power. In the previous work, the evaluation of a mismatching condition over one thermoelectric module was studied [146,147] and the results showed that the non-uniform thermal distribution of TEM reduces the power generation and decreases efficiency.

7. Conclusions

In this paper, the thermoelectric principles, applications, materials, models, and interconnected systems for electric power generation from heat sources have been explained and the recent studies conducted on them have been discussed. Moreover, to address the fundamental issue of energy conversion, special attention was paid to mathematical models and outcomes of these works in terms of their complexity and phenomenological components. Accordingly, comparing the present models for TEG, the complex models considering the mismatching conditions provide more understanding of the thermoelectric systems than the simpler models. Therefore, for future research, improving these models and the development of methodological design systems is recommended to develop more sustainable and efficient infrastructure systems. The literature review presented in this paper shows the tendency of using a TEG system to recover and harvest thermal energy from waste heat sources, but there is not a detailed methodological analysis of the behavior of TEG systems that considers both the thermal dependence properties and side-leg heat losses or the power output in TEM arrays under mismatching thermal conditions considering complex models and power converters, which led to the overestimation of the total power production in TEG systems.

Finally, another promising topic in this field is developing materials with high conversion rates capable of energy harvesting. Recently developed nanostructured materials achieve higher performance by reducing the lattice thermal conductivity and improving electrical transport performance because they have a high potential for further improvements and future applications.

Funding: This research received no external funding, and the APC was funded by Instituto Tecnológico Metropolitano.

Institutional Review Board Statement: Not applicable.

Informed Consent Statement: Not applicable.

Acknowledgments: The author would like to thank to Instituto Tecnológico Metropolitano.

Conflicts of Interest: The author declare no conflict of interest.

References

1. UNFCC (United Nations Framework Convention on Climate Change). *Paris Agreement*; UNFCCC: Bonn, Germany, 2015; p. 29. (In Spanish)
2. Morini, M.; Pinelli, M.; Spina, P.R.; Venturini, M. Optimal allocation of thermal, electric and cooling loads among gener-ation technologies in household applications. *Appl. Energy* **2013**, *112*, 205–214. [CrossRef]
3. Du, W.-J.; Yin, Q.; Cheng, L. Experiments on novel heat recovery systems on rotary kilns. *Appl. Therm. Eng.* **2018**, *139*, 535–541. [CrossRef]
4. Haddad, C.; Périlhon, C.; Danlos, A.; François, M.-X.; Descombes, G. Some Efficient Solutions to Recover Low and Medium Waste Heat: Competitiveness of the Thermoacoustic Technology. *Energy Procedia* **2014**, *50*, 1056–1069. [CrossRef]
5. Montecucco, A.; Buckle, J.R.; Knox, A.R. Solution to the 1-D unsteady heat conduction equation with in-ternal Joule heat generation for thermoelectric devices. *Appl. Therm. Eng.* **2012**, *35*, 177–184. [CrossRef]
6. Wang, X.D.; Huang, Y.X.; Cheng, C.H.; Lin, D.T.; Kang, C.H. A three-dimensional numerical modeling of ther-moelectric device with consideration of coupling of temperature field and electric potential field. *Energy* **2012**, *47*, 488–497. [CrossRef]
7. Enn Velmre, Thomas Johann Seebeck (1770–1831). *Est. J. Eng.* **2007**, *13*, 276–282.
8. Stockolm, J. Générateurs Thermo-Électriques. Journées Electrotechniques du Club EEA. 2003, pp. 15–21. Available online: https://www.researchgate.net/publication/228925386_GENERATION_THERMOELECTRIQUE (accessed on 15 November 2022).

9. Elsheikh, M.H.; Shnawah, D.A.; Sabri, M.F.M.; Said, S.B.M.; Hassan, M.H.; Bashir, M.B.A.; Mohamad, M. A review on thermoelectric renewable energy: Principle parameters that affect their performance. *Renew. Sustain. Energy Rev.* **2014**, *30*, 337–355. [CrossRef]
10. Söylemez, E.; Alpman, E.; Onat, A. Experimental analysis of hybrid household refrigerators including thermoelectric and vapour compression cooling systems. *Int. J. Refrig.* **2018**, *95*, 93–107. [CrossRef]
11. Wang, Y.; Zhang, H.; Hao, H.; Li, H. Performance assessment and parametric study of a hybrid system consisting of an alkali metal thermoelectric converter and an absorption refrigerator. *Energy Convers. Manag.* **2019**, *188*, 346–353. [CrossRef]
12. Zheng, X.; Liu, C.; Yan, Y.; Wang, Q. A review of thermoelectrics research—Recent developments and potentials for sustainable and renewable energy applications. *Renew. Sustain. Energy Rev.* **2014**, *32*, 486–503. [CrossRef]
13. Champier, D. Thermoelectric generators: A review of applications. *Energy Convers. Manag.* **2017**, *140*, 167–181. [CrossRef]
14. Onsager, L. Irreversible Processes. *Phys. Rev.* **1931**, *37–38*, 183–196.
15. Kirschner, I.; Molnár, P. Relation between Curie's principle and Onsager's reciprocity. *Acta Phys. Hung.* **1989**, *66*, 277–287. [CrossRef]
16. Beretta, D.; Neophytou, N.; Hodges, J.M.; Kanatzidis, M.G.; Narducci, D.; Martin-Gonzalez, M.; Beekman, M.; Balke, B.; Cerretti, G.; Tremel, W.; et al. Thermoelectrics: From history, a window to the future. *Mater. Sci. Eng. R Rep.* **2019**, *138*, 100501. [CrossRef]
17. Munera, F. Desarrollo de un Modelo Matemático Fenomenológico que Permita Simular el Comportamiento de Sistemas Termoeléctricos. 2012, p. 98. Available online: https://repositorio.unal.edu.co/handle/unal/11246?show=full (accessed on 15 November 2022).
18. Zhang, M.; Tian, Y.; Xie, H.; Wu, Z.; Wang, Y. Influence of Thomson effect on the thermoelectric generator. *Int. J. Heat Mass Transf.* **2019**, *137*, 1183–1190. [CrossRef]
19. Kaushik, S.C.; Manikandan, S. The influence of Thomson effect in the energy and exergy efficiency of an annular ther-moelectric generator. *Energy Convers. Manag.* **2015**, *103*, 200–207. [CrossRef]
20. Lamba, R.; Kaushik, S. Thermodynamic analysis of thermoelectric generator including influence of Thomson effect and leg geometry configuration. *Energy Convers. Manag.* **2017**, *144*, 388–398. [CrossRef]
21. Tedeschi, S.; Mehnen, J.; Tapoglou, N.; Roy, R. Secure IoT Devices for the Maintenance of Machine Tools. *Procedia CIRP* **2016**, *59*, 150–155. [CrossRef]
22. Cataldo, R.L.; Bennett, G.L. U.S. Space Radioisotope Power Systems and Applications: Past, Present and Future. 2011. Available online: https://ntrs.nasa.gov/citations/20120000731 (accessed on 15 November 2022).
23. Shi, L.; Shu, G.; Tian, H.; Deng, S. A review of modified Organic Rankine cycles (ORCs) for internal combustion engine waste heat recovery (ICE-WHR). *Renew. Sustain. Energy Rev.* **2018**, *92*, 95–110. [CrossRef]
24. Shu, G.; Yu, Z.; Tian, H.; Liu, P.; Xu, Z. Potential of the transcritical Rankine cycle using CO_2-based binary zeotropic mixtures for engine's waste heat recovery. *Energy Convers. Manag.* **2018**, *174*, 668–685. [CrossRef]
25. Zhi, L.-H.; Hu, P.; Chen, L.-X.; Zhao, G. Parametric analysis and optimization of transcritical-subcritical dual-loop organic Rankine cycle using zeotropic mixtures for engine waste heat recovery. *Energy Convers. Manag.* **2019**, *195*, 770–787. [CrossRef]
26. Ramírez, R.; Gutiérrez, A.S.; Eras, J.J.C.; Valencia, K.; Hernández, B.; Forero, J.D. Evaluation of the energy recovery potential of thermoelectric generators in diesel engines. *J. Clean. Prod.* **2019**, *241*, 118412. [CrossRef]
27. Khalil, H.; Hassan, H. Enhancement thermoelectric generators output power from heat recovery of chimneys by using flaps. *J. Power Sources* **2019**, *443*, 227266. [CrossRef]
28. Aranguren, P.; Astrain, D.; Rodríguez, A.; Martínez, A. Experimental investigation of the applicability of a thermoelectric generator to recover waste heat from a combustion chamber. *Appl. Energy* **2015**, *152*, 121–130. [CrossRef]
29. Luo, Q.; Li, P.; Cai, L.; Zhou, P.; Tang, D.; Zhai, P.; Zhang, Q. A Thermoelectric Waste-Heat-Recovery System for Portland Cement Rotary Kilns. *J. Electron. Mater.* **2015**, *44*, 1750–1762. [CrossRef]
30. Kaibe, H.; Makino, K.; Kajihara, T.; Fujimoto, S.; Hachiuma, H. Thermoelectric generating system attached to a carburizing furnace at Komatsu Ltd. *Awazu Plant.* **2012**, *1449*, 524. [CrossRef]
31. Kuroki, T.; Kabeya, K.; Makino, K.; Kajihara, T.; Kaibe, H.; Hachiuma, H.; Matsuno, H.; Fujibayashi, A. Thermoelectric Generation Using Waste Heat in Steel Works. *J. Electron. Mater.* **2014**, *43*, 2405–2410. [CrossRef]
32. Kuroki, T.; Murai, R.; Makino, K.; Nagano, K.; Kajihara, T.; Kaibe, H.; Hachiuma, H.; Matsuno, H. Research and Development for Thermoelectric Generation Technology Using Waste Heat from Steelmaking Process. *J. Electron. Mater.* **2015**, *44*, 2151–2156. [CrossRef]
33. Kajihara, T.; Makino, K.; Lee, Y.H.; Kaibe, H.; Hachiuma, H. Study of Thermoelectric Generation Unit for Radiant Waste Heat. *Mater. Today Proc.* **2015**, *2*, 804–813. [CrossRef]
34. Microplet. mva-002 @ www.micropelt.com. 2020. Available online: http://www.micropelt.com/en/products/mva-002.html (accessed on 15 November 2022).
35. Perpetua, Getting Started | Perpetua Power Source Technologies, Inc. Available online: https://perpetuapower.com/getting-started/ (accessed on 14 June 2020).
36. Kim, Y.J.; Gu, H.M.; Kim, C.S.; Choi, H.; Lee, G.; Kim, S.; Yi, K.K.; Lee, S.G.; Cho, B.J. High-performance self-powered wireless sensor node driven by a flexible thermoelectric generator. *Energy* **2018**, *162*, 526–533. [CrossRef]
37. Milić, D.; Prijić, A.; Vračar, L.; Prijić, Z. Characterization of commercial thermoelectric modules for application in energy harvesting wireless sensor nodes. *Appl. Therm. Eng.* **2017**, *121*, 74–82. [CrossRef]

38. Guan, M.; Wang, K.; Xu, D.; Liao, W.-H. Design and experimental investigation of a low-voltage thermoelectric energy harvesting system for wireless sensor nodes. *Energy Convers. Manag.* **2017**, *138*, 30–37. [CrossRef]
39. Karthikeyan, V.; Surjadi, J.U.; Wong, J.C.; Kannan, V.; Lam, K.-H.; Chen, X.; Lu, Y.; Roy, V.A. Wearable and flexible thin film thermoelectric module for multi-scale energy harvesting. *J. Power Sources* **2019**, *455*, 227983. [CrossRef]
40. Wang, Y.; Shi, Y.; Mei, D.; Chen, Z. Wearable thermoelectric generator for harvesting heat on the curved human wrist. *Appl. Energy* **2017**, *205*, 710–719. [CrossRef]
41. Hyland, M.; Hunter, H.; Liu, J.; Veety, E.; Vashaee, D. Wearable thermoelectric generators for human body heat harvesting. *Appl. Energy* **2016**, *182*, 518–524. [CrossRef]
42. Cao, J.; Querales, J.; Fahy, S.; Savić, I. Thermally induced band gap increase and high thermoelectric figure of merit of n-type PbTe. *Mater. Today Phys.* **2019**, *12*, 100172. [CrossRef]
43. Wu, Y.; Zhang, H.; Zuo, L. Thermoelectric energy harvesting for the gas turbine sensing and monitoring system. *Energy Convers. Manag.* **2018**, *157*, 215–223. [CrossRef]
44. Janak, L.; Ancik, Z.; Vetiska, J.; Hadas, Z. Thermoelectric Generator Based on MEMS Module as an Electric Power Backup in Aerospace Applications. *Mater. Today Proc.* **2015**, *2*, 865–870. [CrossRef]
45. Kousksou, T.; Bédécarrats, J.P.; Champier, D.; Pignolet, P.; Brillet, C. Numerical study of thermoelectric power generation for an helicopter conical nozzle. *J. Power Sources* **2011**, *196*, 4026–4032. [CrossRef]
46. Kristiansen, N.R.; Nielsen, H.K. Potential for Usage of Thermoelectric Generators on Ships. *J. Electron. Mater.* **2010**, *39*, 1746–1749. [CrossRef]
47. Kristiansen, N.R.; Snyder, J.; Nielsen, H.K.; Rosendahl, L. Waste Heat Recovery from a Marine Waste Incinerator Using a Thermoelectric Generator. *J. Electron. Mater.* **2012**, *41*, 1024–1029. [CrossRef]
48. Eddine, A.N.; Chalet, D.; Faure, X.; Aixala, L.; Chessé, P. Optimization and characterization of a thermoelectric gen-erator prototype for marine engine application. *Energy* **2018**, *143*, 682–695. [CrossRef]
49. Zhu, W.; Huang, Z.; Chu, M.; Li, S.; Zhang, Y.; Ao, W.; Wang, R.; Luo, J.; Liu, F.; Xiao, Y.; et al. Enhanced thermoelectric performance through optimizing structure of anionic framework in AgCuTe-based materials. *Chem. Eng. J.* **2020**, *386*, 123917. [CrossRef]
50. Li, G.; He, J.; An, Q.; Morozov, S.; Hao, S.; Zhai, P.; Zhang, Q.; Goddard, W.A.; Snyder, G.J. Dramatically reduced lattice thermal conductivity of Mg2Si thermoelectric material from nanotwinning. *Acta Mater.* **2019**, *169*, 9–14. [CrossRef]
51. Qin, D.; Cui, B.; Meng, X.; Qin, P.; Xie, L.; Zhang, Q.; Liu, W.; Cao, J.; Cai, W.; Sui, J. High thermoelectric performance from high carrier mobility and reduced lattice thermal conductivity in Ba, Yb double-filled Skutterudites. *Mater. Today Phys.* **2019**, *8*, 128–137. [CrossRef]
52. Hori, T. Role of geometry and surface roughness in reducing phonon mean free path and lattice thermal conductivity of modulated nanowires. *Int. J. Heat Mass Transf.* **2020**, *156*, 119818. [CrossRef]
53. Huang, L.; Guo, J.; Ge, Z.H.; Jiang, Y.; Feng, J. Significantly reduced lattice thermal conductivity and enhanced thermoe-lectric performance of In_2O_3 $(ZnO)_3$ ceramics by Ga_2O_3 doping. *J. Solid State Chem.* **2020**, *281*, 121022. [CrossRef]
54. Balandin, A.A.; Nika, D.L. Phononics in low-dimensional materials Phonons—Quanta of crystal lattice vibrations—Reveal themselves in all. *Mater. Today* **2012**, *15*, 266–275. [CrossRef]
55. Rittiruam, M.; Yangthaisong, A.; Seetawan, T. Reduced lattice thermal conductivity of Ti-site substituted transition metals Ti1-XTMXNiSn: A quasi-harmonic Debye model study. *Chin. J. Phys.* **2018**, *57*, 393–402. [CrossRef]
56. Zhang, Z.; Hu, S.; Nakayama, T.; Chen, J.; Li, B. Reducing lattice thermal conductivity in schwarzites via engineering the hybridized phonon modes. *Carbon* **2018**, *139*, 289–298. [CrossRef]
57. Crane, D.T.; Jackson, G.S. Optimization of cross flow heat exchangers for thermoelectric waste heat recovery. *Energy Convers. Manag.* **2004**, *45*, 1565–1582. [CrossRef]
58. Chen, J.; Wu, C. Analysis on the Performance of a Thermoelectric Generator. *J. Energy Resour. Technol.* **1999**, *122*, 61–63. [CrossRef]
59. Culebras, M.; Igual-Muñoz, A.M.; Rodríguez-Fernández, C.; Gómez-Gómez, M.I.; Gómez, C.; Cantarero, A. Manufacturing Te/PEDOT Films for Thermoelectric Applications. *ACS Appl. Mater. Interfaces* **2017**, *9*, 20826–20832. [CrossRef] [PubMed]
60. Sabarinathan, M.; Omprakash, M.; Harish, S.; Navaneethan, M.; Archana, J.; Ponnusamy, S.; Ikeda, H.; Takeuchi, T.; Muthamizhchelvan, C.; Hayakawa, Y. Enhancement of power factor by energy filtering effect in hierarchical BiSbTe3 nanostructures for thermoelectric applications. *Appl. Surf. Sci.* **2017**, *418*, 246–251. [CrossRef]
61. Ai, X.; Hou, D.; Liu, X.; Gu, S.; Wang, L.; Jiang, W. Enhanced thermoelectric performance of PbTe-based nanocomposites through element doping and SiC nanoparticles dispersion. *Scr. Mater.* **2020**, *179*, 86–91. [CrossRef]
62. Cai, B.; Hu, H.; Zhuang, H.-L.; Li, J.-F. Promising materials for thermoelectric applications. *J. Alloys Compd.* **2019**, *806*, 471–486. [CrossRef]
63. Chang, C.; Wu, M.; He, D.; Pei, Y.; Wu, C.-F.; Wu, X.; Yu, H.; Zhu, F.; Wang, K.; Chen, Y.; et al. 3D charge and 2D phonon transports leading to high out-of-plane ZT in n-type SnSe crystals. *Science* **2018**, *360*, 778–783. [CrossRef]
64. Poudel, B.; Hao, Q.; Ma, Y.; Lan, Y.; Minnich, A.; Yu, B.; Yan, X.; Wang, D.; Muto, A.; Vashaee, D.; et al. High-Thermoelectric Performance of Nanostructured Bismuth Antimony Telluride Bulk Alloys. *Science* **2008**, *320*, 634–638. [CrossRef]
65. Xie, W.; He, J.; Kang, H.J.; Tang, X.; Zhu, S.; Laver, M.; Wang, S.; Copley, J.R.; Brown, C.M.; Zhang, Q.; et al. Identifying the specific nanostructures responsible for the high thermoelectric performance of (Bi,Sb)2Te3 nanocomposites. *Nano Lett.* **2010**, *10*, 3283–3289. [CrossRef]

66. Zhu, T.; Xu, Z.; He, J.; Shen, J.; Zhu, S.; Hu, L.; Tritt, T.M.; Zhao, X. Hot deformation induced bulk nanostructuring of unidirectionally grown p-type (Bi,Sb)2Te3 thermoelectric materials. *J. Mater. Chem. A* **2013**, *1*, 11589–11594. [CrossRef]
67. Kim, S.I.; Lee, K.H.; Mun, H.A.; Kim, H.S.; Hwang, S.W.; Roh, J.W.; Yang, D.J.; Shin, W.H.; Li, X.S.; Lee, Y.H.; et al. Dense dislocation arrays embedded in grain boundaries for high-performance bulk thermoelectrics. *Science* **2015**, *348*, 109–114. [CrossRef] [PubMed]
68. Kim, K.T.; Min, T.S.; Kim, S.-D.; Choi, E.-A.; Kim, D.W.; Choi, S.-Y. Strain-mediated point defects in thermoelectric p-type bismuth telluride polycrystalline. *Nano Energy* **2018**, *55*, 486–493. [CrossRef]
69. Zhu, T.; Xu, Z.; He, J.; Shen, J.; Zhu, S.; Hu, L.; Tritt, T.M.; Zhao, X. Enhancement of Thermoelectric of the Electronic Density of States. *Science* **2008**, *321*, 1457–1461.
70. Sun, H.; Yu, F.; Zhao, P.; Wang, B.; Cai, B.; Zhang, L.; Yu, D.; Tian, Y.; Xu, B. Thermoelectric performance of single elemental doped n-type PbTe regulated by carrier concentration. *J. Alloys Compd.* **2019**, *787*, 180–185. [CrossRef]
71. Li, Z.Y.; Li, J.F. Fine-Grained and nanostructured AgPbmSbTem+2 alloys with high thermoelectric figure of merit at medium temperature. *Adv. Energy Mater.* **2014**, *4*, 1300937. [CrossRef]
72. Cai, B.; Li, J.; Sun, H.; Zhang, L.; Xu, B.; Hu, W.; Yu, D.; He, J.; Zhao, Z.; Liu, Z.; et al. Enhanced thermoelectric performance of Na-doped PbTe synthesized under high pressure. *Sci. China Mater.* **2018**, *61*, 1218–1224. [CrossRef]
73. Wu, Y.; Chen, Z.; Nan, P.; Xiong, F.; Lin, S.; Zhang, X.; Chen, Y.; Chen, L.; Ge, B.; Pei, Y. Lattice Strain Advances Thermoelectrics. *Joule* **2019**, *3*, 1276–1288. [CrossRef]
74. Yu, B.; Zebarjadi, M.; Wang, H.; Lukas, K.; Wang, H.; Wang, D.; Opeil, C.; Dresselhaus, M.; Chen, G.; Ren, Z. Enhancement of Thermoelectric Properties by Modulation-Doping in Silicon Germanium Alloy Nanocomposites. *Nano Lett.* **2012**, *12*, 2077–2082. [CrossRef]
75. Usenko, A.; Moskovskikh, D.; Gorshenkov, M.; Voronin, A.; Stepashkin, A.; Kaloshkin, S.; Arkhipov, D.; Khovaylo, V. Scripta Materialia nanostructured spark plasma sintered alloys with embedded SiO_2 nanoinclusions. *Scr. Maeterialia* **2017**, *127*, 63–67. [CrossRef]
76. Rogl, G.; Grytsiv, A.; Rogl, P.; Peranio, N.; Bauer, E.; Zehetbauer, M.; Eibl, O. n-Type skutterudites (R,Ba,Yb)yCo4Sb12 (R = Sr, La, Mm, DD, SrMm, SrDD) approaching ZT 2.0. *Acta Mater.* **2014**, *29*, 209–214. [CrossRef]
77. Liu, W.; Tan, X.; Yin, K.; Liu, H.; Tang, X.; Shi, J.; Zhang, Q.; Uher, C. Convergence of conduction bands as a means of enhancing thermoelectric performance of n-type Mg 2Si 1-xSn x solid solutions. *Phys. Rev. Lett.* **2012**, *108*, 166601. [CrossRef] [PubMed]
78. Zhang, Q.; He, J.; Zhu, T.J.; Zhang, S.N.; Zhao, X.B.; Tritt, T.M. High figures of merit and natural nanostructures in Mg2Si 0.4Sn0.6 based thermoelectric materials. *Appl. Phys. Lett.* **2008**, *93*, 102109. [CrossRef]
79. Zhao, H.; Cao, B.; Li, S.; Liu, N.; Shen, J.; Li, S.; Jian, J.; Gu, L.; Pei, Y.; Snyder, G.J.; et al. Engineering the Thermoelectric Transport in Half-Heusler Materials through a Bottom-Up Nanostructure Synthesis. *Adv. Energy Mater.* **2017**, *7*, 1700446. [CrossRef]
80. Snyder, G.J.; Christensen, M.; Nishibori, E.; Caillat, T.; Iversen, B. Disordered zinc in Zn4Sb3 with phonon-glass and electron-crystal thermoelectric properties. *Nat. Mater.* **2004**, *3*, 458–463. [CrossRef] [PubMed]
81. Chen, X.; Wu, H.; Cui, J.; Xiao, Y.; Zhang, Y.; He, J.; Chen, Y.; Cao, J.; Cai, W.; Pennycook, S.J.; et al. Extraordinary thermoelectric performance in n-type manganese doped Mg3Sb2 Zintl: High band degeneracy, tuned carrier scattering mechanism and hierarchical microstructure. *Nano Energy* **2018**, *52*, 246–255. [CrossRef]
82. Wei, W.; Chang, C.; Yang, T.; Liu, J.; Tang, H.; Zhang, J.; Li, Y.; Xu, F.; Zhang, Z.; Li, J.-F.; et al. Achieving High Thermoelectric Figure of Merit in Polycrystalline SnSe via Introducing Sn Vacancies. *J. Am. Chem. Soc.* **2018**, *140*, 499–505. [CrossRef]
83. Nunna, R.; Qiu, P.; Yin, M.; Chen, H.; Hanus, R.; Song, Q.; Zhang, T.; Chou, M.-Y.; Agne, M.T.; He, J.; et al. Ultrahigh thermoelectric performance in Cu2Se-based hybrid materials with highly dispersed molecular CNTs. *Energy Environ. Sci.* **2017**, *10*, 1928–1935. [CrossRef]
84. Chen, X.; Dai, W.; Wu, T.; Luo, W.; Yang, J.; Jiang, W.; Wang, L. Thin Film Thermoelectric Materials: Classification, Characterization, and Potential for Wearable Applications. *Coatings* **2018**, *8*, 244. [CrossRef]
85. Yang, S.; Chung, L.; Wang, H. Review of Polysilicon Thermoelectric Energy Generators. *Sens. Actuators A Phys.* **2022**, *346*, 113890. [CrossRef]
86. Nascimento, J.C.A.D.; Kerrigan, A.; Hasnip, P.J.; Lazarov, V.K. Significant improvement of the Seebeck coefficient of Fe_2VAl with antisite defects. *Mater. Today Commun.* **2022**, *31*, 103510. [CrossRef]
87. Gao, N.; Zhu, B.; Wang, X.-Y.; Yu, Y.; Zu, F.-Q. Simultaneous optimization of Seebeck, electrical and thermal conductivity in free-solidified Bi0.4Sb1.6Te3 alloy via liquid-state manipulation. *J. Mater. Sci.* **2018**, *53*, 9107–9116. [CrossRef]
88. Saberi, Y.; Sajjadi, S.A. A comprehensive review on the effects of doping process on the thermoelectric properties of Bi2Te3 based alloys. *J. Alloys Compd.* **2022**, *904*, 163918. [CrossRef]
89. Zhang, Y.; Park, S.-J. Flexible Organic Thermoelectric Materials and Devices for Wearable Green Energy Harvesting. *Polymers* **2019**, *11*, 909. [CrossRef] [PubMed]
90. Liu, W.; Yan, X.; Chen, G.; Ren, Z. Recent advances in thermoelectric nanocomposites. *Nano Energy* **2012**, *1*, 42–56. [CrossRef]
91. Xiao, Y.; Wu, Y.; Nan, P.; Dong, H.; Chen, Z.; Chen, Z.; Gu, H.; Ge, B.; Li, W.; Pei, Y. Cu Interstitials Enable Carriers and Dislocations for Thermoelectric Enhancements in n-PbTe0.75Se0.25. *Chemistry* **2020**, *6*, 523–537. [CrossRef]
92. Liu, H.-T.; Sun, Q.; Zhong, Y.; Deng, Q.; Gan, L.; Lv, F.-L.; Shi, X.-L.; Chen, Z.-G.; Ang, R. High-performance in n-type PbTe-based thermoelectric materials achieved by synergistically dynamic doping and energy filtering. *Nano Energy* **2022**, *91*, 106706. [CrossRef]

93. Yang, G.; Sang, L.; Mitchell, D.R.; Yun, F.F.; See, K.W.; Ahmed, A.J.; Sayyar, S.; Bake, A.; Liu, P.; Chen, L.; et al. Enhanced thermoelectric performance and mechanical strength of n-type BiTeSe materials produced via a composite strategy. *Chem. Eng. J.* **2022**, *428*, 131205. [CrossRef]
94. Mo, X.; Liao, J.; Yuan, G.; Zhu, S.; Lei, X.; Huang, L.; Zhang, Q.; Wang, C.; Ren, Z. High thermoelectric performance at room temperature of n-type Mg3Bi2-based materials by Se doping. *J. Magnes. Alloy.* **2022**, *10*, 1024–1032. [CrossRef]
95. Yang, L.; Chen, Z.-G.; Hong, M.; Wang, L.; Kong, D.; Huang, L.; Han, G.; Zou, Y.; Dargusch, M.; Zou, J. n-type Bi-doped PbTe Nanocubes with Enhanced Thermoelectric Performance. *Nano Energy* **2017**, *31*, 105–112. [CrossRef]
96. Lee, M.H.; Yun, J.H.; Kim, G.; Lee, J.E.; Park, S.D.; Reith, H.; Schierning, G.; Nielsch, K.; Ko, W.; Li, A.P.; et al. Synergetic Enhancement of Thermoelectric Performance by Selective Charge Anderson Localiza-tion-Delocalization Transition in n-Type Bi-Doped PbTe/Ag 2 Te Nanocomposite. *ACS Nano* **2019**, *13*, 3806–3815. [CrossRef]
97. Lu, Y.; Wang, J.-Y.; Pei, J. Strategies To Enhance the Conductivity of n-Type Polymer Thermoelectric Materials. *Chem. Mater.* **2019**, *31*, 6412–6423. [CrossRef]
98. Liu, J.; Qiu, L.; Alessandri, R.; Qiu, X.; Portale, G.; Dong, J.; Talsma, W.; Ye, G.; Sengrian, A.A.; de Souza, P.C.T.; et al. Enhancing Molecular n-Type Doping of Donor-Acceptor Copolymers by Tailoring Side Chains. *Adv. Mater.* **2018**, *30*, 1704630. [CrossRef] [PubMed]
99. Wang, S.; Zuo, G.; Kim, J.; Sirringhaus, H. Progress of Conjugated Polymers as Emerging Thermoelectric Materials. *Prog. Polym. Sci.* **2022**, *129*, 101548. [CrossRef]
100. Zhu, M.; Chang, Z.; Wu, S.; Sun, Y.; Li, Y.; Jin, Y.; Zou, Y.; Sun, Y.; Xu, W.; Zhu, D. Optimization of thermoelectric performances of conjugated polymers containing Trans-1,2-di(2-thienyl)ethylene subunits via structural modulation and doping engineering. *Org. Electron.* **2022**, *111*, 106671. [CrossRef]
101. Yang, C.-Y.; Ding, Y.-F.; Huang, D.; Wang, J.; Yao, Z.-F.; Huang, C.-X.; Lu, Y.; Un, H.-I.; Zhuang, F.-D.; Dou, J.-H.; et al. A thermally activated and highly miscible dopant for n-type organic thermoelectrics. *Nat. Commun.* **2020**, *11*, 3292. [CrossRef]
102. Lee, S.; Kim, S.; Pathak, A.; Tripathi, A.; Qiao, T.; Lee, Y.; Lee, H.; Woo, H.Y. Recent Progress in Organic Thermoelectric Materials and Devices. *Macromol. Res.* **2020**, *28*, 531–552. [CrossRef]
103. Wang, L.; Yao, Q.; Xiao, J.; Zeng, K.; Qu, S.; Shi, W.; Wang, Q.; Chen, L. Engineered Molecular Chain Ordering in Single-Walled Carbon Nanotubes/Polyaniline Composite Films for High-Performance Organic Thermoelectric Materials. *Chem. Asian J.* **2016**, *11*, 1804–1810. [CrossRef]
104. Sun, Y.; Qiu, L.; Tang, L.; Geng, H.; Wang, H.; Zhang, F.; Huang, D.; Xu, W.; Yue, P.; Guan, Y.-S.; et al. Flexible n-Type High-Performance Thermoelectric Thin Films of Poly(nickel-ethylenetetrathiolate) Prepared by an Electrochemical Method. *Adv. Mater.* **2016**, *28*, 3351–3358. [CrossRef]
105. Li, Y.; Gao, C.-Y.; Fan, X.-H.; Yang, L.-M. Two-step electrochemical modification for improving thermoelectric performance of polypyrrole films. *Synth. Met.* **2021**, *282*, 116949. [CrossRef]
106. Almasoudi, M.; Zoromba, M.S.; Abdel-Aziz, M.; Bassyouni, M.; Alshahrie, A.; Abusorrah, A.M.; Salah, N. Optimization preparation of one-dimensional polypyrrole nanotubes for enhanced thermoelectric performance. *Polymer* **2021**, *228*, 123950. [CrossRef]
107. Zhang, R.; Zhang, S.; Yin, Q.; Jiang, B.; Wang, Y.; Du, K.; Yin, Q. Polyaniline doped with copper phthalocyanine disulfonic acid and their unique thermoelectric performance. *Polymer* **2022**, *261*, 125337. [CrossRef]
108. Abd-Elsalam, A.; Badr, H.O.; Abdel-Rehim, A.A.; El-Mahallawi, I.S. Structure and thermoelectric behavior of polyaniline-based/CNT-composite. *Curr. Appl. Phys.* **2022**, *36*, 88–92. [CrossRef]
109. Huang, J.; Liu, X.; Du, Y. Fabrication of free-standing flexible and highly efficient carbon nanotube film/PEDOT: PSS thermoelectric composites. *J. Materiomics* **2022**, *8*, 1213–1217. [CrossRef]
110. Liu, L.; Chen, J.; Liang, L.; Deng, L.; Chen, G. A PEDOT:PSS thermoelectric fiber generator. *Nano Energy* **2022**, *102*, 107678. [CrossRef]
111. Liu, D.; Yan, Z.; Zhao, Y.; Zhang, Z.; Zheng, Y.; Zhang, B.; Shi, P.; Xue, C. Enhanced performance of SnSe/PEDOT: PSS composite films by MWCNTs for flexible thermoelectric power generator. *J. Alloys Compd.* **2022**, *898*, 162844. [CrossRef]
112. Wang, X.; Wang, H.; Liu, B. Carbon Nanotube-Based Organic Thermoelectric Materials for Energy Harvesting. *Polymers* **2018**, *10*, 1196. [CrossRef] [PubMed]
113. Blackburn, J.L.; Ferguson, A.J.; Cho, C.; Grunlan, J.C. Carbon-Nanotube-Based Thermoelectric Materials and Devices. *Adv. Mater.* **2018**, *30*, 1704386. [CrossRef]
114. Elsehly, E.; Ibrahim, E.; El-Hadek, M.A.; El-Khouly, A.; Khovaylo, V.; Elqahtani, Z.; Chechenin, N.; Adam, A. Annealing effect on the thermoelectric properties of multiwall carbon nanotubes. *Phys. E Low-Dimens. Syst. Nanostructures* **2023**, *146*, 115566. [CrossRef]
115. Tzeng, S.-C.; Jeng, T.-M.; Lin, Y.-L. Parametric study of heat-transfer design on the thermoelectric generator system. *Int. Commun. Heat Mass Transf.* **2014**, *52*, 97–105. [CrossRef]
116. Twaha, S.; Zhu, J.; Yan, Y.; Li, B. A comprehensive review of thermoelectric technology: Materials, applications, modelling and performance improvement. *Renew. Sustain. Energy Rev.* **2016**, *65*, 698–726. [CrossRef]

117. Ge, Z.; Jin, L.; Yang, C. Microfluidic concentration of sample solutes using Joule heating effects under a combined AC and DC electric field. *Int. J. Heat Mass Transf.* **2015**, *85*, 158–165. [CrossRef]
118. Fraisse, G.; Ramousse, J.; Sgorlon, D.; Goupil, C. Comparison of different modeling approaches for thermoelectric elements. *Energy Convers. Manag.* **2013**, *65*, 351–356. [CrossRef]
119. Siddique, A.R.M.; Rabari, R.; Mahmud, S.; Van Heyst, B. Thermal energy harvesting from the human body using flexible thermoelectric generator (FTEG) fabricated by a dispenser printing technique. *Energy* **2016**, *115*, 1081–1091. [CrossRef]
120. Chen, L.; Meng, F.; Sun, F. Effect of heat transfer on the performance of thermoelectric generator-driven thermoelectric refrigerator system. *Cryogenics* **2012**, *52*, 58–65. [CrossRef]
121. Chen, W.H.; Wu, P.H.; Wang, X.D.; Lin, Y.L. Power output and efficiency of a thermoelectric generator under temper-ature control. *Energy Convers. Manag.* **2016**, *127*, 404–415. [CrossRef]
122. Lee, H. The Thomson effect and the ideal equation on thermoelectric coolers. *Energy* **2013**, *56*, 61–69. [CrossRef]
123. Chakraborty, A.; Saha, B.; Koyama, S.; Ng, K.C. Thermodynamic modelling of a solid state thermoelectric cooling device: Temperature–entropy analysis. *Int. J. Heat Mass Transf.* **2006**, *49*, 3547–3554. [CrossRef]
124. Chakraborty, A.; Ng, K.C. Thermodynamic formulation of temperature–entropy diagram for the transient operation of a pulsed thermoelectric cooler. *Int. J. Heat Mass Transf.* **2006**, *49*, 1845–1850. [CrossRef]
125. Kanimba, E.; Tian, Z. A new dimensionless number for thermoelectric generator performance. *Appl. Therm. Eng.* **2019**, *152*, 858–864. [CrossRef]
126. Kim, S. Analysis and modeling of effective temperature differences and electrical parameters of thermoelectric generators. *Appl. Energy* **2013**, *102*, 1458–1463. [CrossRef]
127. Rana, S.; Orr, B.; Iqbal, A.; Ding, L.C.; Akbarzadeh, A.; Date, A. Modelling and Optimization of Low-temperature Waste Heat Thermoelectric Generator System. *Energy Procedia* **2017**, *110*, 196–201. [CrossRef]
128. Mahmoudinezhad, S.; Rezania, A.; Ranjbar, A.A.; Rosendahl, L.A. Transient behavior of the thermoelectric generators to the load change; an experimental investigation. *Energy Procedia* **2018**, *147*, 537–543. [CrossRef]
129. De Aloysio, G.; D'Alessandro, G.; de Monte, F. An analytical solution for the hyperbolic unsteady thermal behaviour of micro-thermoelectric coolers with a suddenly time-dependent heat generation. *Int. J. Heat Mass Transf.* **2016**, *95*, 972–983. [CrossRef]
130. Cheng, C.-H.; Huang, S.-Y.; Cheng, T.-C. A three-dimensional theoretical model for predicting transient thermal behavior of thermoelectric coolers. *Int. J. Heat Mass Transf.* **2010**, *53*, 2001–2011. [CrossRef]
131. Musland, L.; Flage-Larsen, E. Thermoelectric transport calculations using the Landauer approach, ballistic quantum transport simulations, and the Buttiker approximation. *Comput. Mater. Sci.* **2017**, *132*, 146–157. [CrossRef]
132. Yamashita, O. Effect of linear and non-linear components in the temperature dependences of thermoelectric properties on the energy conversion efficiency. *Energy Convers. Manag.* **2009**, *50*, 1968–1975. [CrossRef]
133. Wee, D. Uncertainty and sensitivity of the maximum power in thermoelectric generation with temperature-dependent ma-terial properties: An analytic polynomial chaos approach. *Energy Convers. Manag.* **2018**, *157*, 103–110. [CrossRef]
134. Ju, C.; Dui, G.; Zheng, H.H.; Xin, L. Revisiting the temperature dependence in material properties and performance of thermo-electric materials. *Energy* **2017**, *124*, 249–257. [CrossRef]
135. Lee, H.; Sharp, J.; Stokes, D.; Pearson, M.; Priya, S. Modeling and analysis of the effect of thermal losses on thermoelectric generator performance using effective properties. *Appl. Energy* **2018**, *211*, 987–996. [CrossRef]
136. Zhang, T. Effects of Temperature-Dependent Material Properties on Temperature Variation in a Thermoelement. *J. Electron. Mater.* **2015**, *44*, 3612–3620. [CrossRef]
137. Kanimba, E.; Pearson, M.; Sharp, J.; Stokes, D.; Priya, S.; Tian, Z. A modeling comparison between a two-stage and three-stage cascaded thermoelectric generator. *J. Power Sources* **2017**, *365*, 266–272. [CrossRef]
138. Montecucco, A.; Siviter, J.; Knox, A.R. The effect of temperature mismatch on thermoelectric generators electrically connected in series and parallel. *Appl. Energy* **2014**, *123*, 47–54. [CrossRef]
139. Belboula, A.; Taleb, R.; Bachir, G.; Chabni, F. *Comparative Study of Maximum Power Point Tracking Algorithms for Thermoelectric Generator*; Springer: Berlin/Heidelberg, Germany, 2019; Volume 62, pp. 329–338. [CrossRef]
140. Sera, D.; Kerekes, T.; Teodorescu, R.; Blaabjerg, F. Improved MPPT Algorithms for Rapidly Changing Environmental Conditions. In Proceedings of the 2006 12th International Power Electronics and Motion Control Conference, Portoroz, Slovenia, 10 February 2009; pp. 1614–1619. Available online: https://ieeexplore.ieee.org/document/4778635 (accessed on 14 June 2020). [CrossRef]
141. Podder, A.K.; Roy, N.K.; Pota, H.R. MPPT methods for solar PV systems: A critical review based on tracking nature. *IET Renew. Power Gener.* **2019**, *13*, 1615–1632. [CrossRef]
142. Satpathy, P.R.; Sharma, R. RETRACTED: Power recovery and equalization in partially shaded photovoltaic strings by an efficient switched capacitor converter. *Energy Convers. Manag.* **2019**, *203*, 112258. [CrossRef]
143. Tofoli, F.L.; de Castro Pereira, D.; de Paula, W.J. Comparative Study of Maximum Power Point Tracking Techniques for Photovoltaic Systems. *Int. J. Photoenergy* **2015**, *2015*, 812582. [CrossRef]
144. Belhachat, F.; Larbes, C. A review of global maximum power point tracking techniques of photovoltaic system under partial shading conditions. *Renew. Sustain. Energy Rev.* **2018**, *92*, 513–553. [CrossRef]
145. Tang, Z.; Deng, Y.; Su, C.; Shuai, W.; Xie, C. A research on thermoelectric generator's electrical performance under temperature mismatch conditions for automotive waste heat recovery system. *Case Stud. Therm. Eng.* **2015**, *5*, 143–150. [CrossRef]

146. Sanin-Villa, D.; Monsalve-Cifuentes, O.D.; Henao-Bravo, E.E. Evaluation of Thermoelectric Generators under Mismatching Conditions. *Energies* **2021**, *14*, 8016. [CrossRef]
147. Sanin-Villa, D.; Monsalve-Cifuentes, O.D.; Del Rio, J.S. Early fever detection on COVID-19 infection using thermoelectric module generators. *Int. J. Electr. Comput. Eng.* **2021**, *11*, 3828–3837. [CrossRef]